Polyaminoacid-Induced Growth of Metal Nanoparticles on Layer-by-Layer Templates

Eugenia Kharlampieva,[†] Joseph M. Slocik,[‡] Taisia Tsukruk,[†] Rajesh R. Naik,[‡] and Vladimir V. Tsukruk*,[†]

School of Materials Science and Engineering, Georgia Institute of Technology, Atlanta, Georgia 30332, and Air Force Research Laboratory, Materials and Manufacturing Directorate, Wright-Patterson Air Force Base, Dayton, Ohio 45433

Received May 30, 2008. Revised Manuscript Received July 8, 2008

We report on preparation of redox-active nanoscale layer-by-layer (LbL) films with polyaminoacid-decorated surfaces that serve for both nucleation and growth of uniformly distributed gold nanoparticles at ambient conditions. We found that a poly-L-tyrosine (pTyr), a synthetic polyaminoacid, was able to direct nanoparticle formation to solid, flexible, and patterned surfaces preventing particle agglomeration. The gold particles were 8 ± 2 nm in diameter, surrounded by 3−6 nm polyaminoacid shell, and confined to the topmost polyaminoacid layer. The reported results on bioinspired gold formation can be readily expanded to any inorganic-selective surface and provide a simple, robust, and nontoxic method to obtain nonaggregated inorganic nanoparticles at ambient conditions.

Introduction

During the past years, research on directed assembly of metal nanoparticles has become a focus of intense studies because of their unique optical, electrical, and other properties.[1,2] In this respect, bioassisted nanoparticle synthesis is an elegant way to obtain metal nanoparticles and corresponding hybrid nanomaterials (organic−inorganic) because the method not only allows us to control nanoparticle shapes, morphologies, and sizes but also involves ambient temperature, nontoxic solvents, and biocompatible templates.[3−5] For example, peptides and proteins that can specifically bind to a certain inorganic surface have been recently found as new molecular templates to obtain silver, platinum, gold, and magnetic nanoparticles, mostly because of the efficient stabilizing activity of the biomolecules in solutions.[6−10] Peptide-mediated synthesis was also applied to multicomponent catalytically efficient gold/palladium bimetallic nanoparticles,[11,12] ferromagnetic FePt nanoparticles,[13] and the complexes of gold nanoparticles with quantum dots.[14]

In addition, some biomolecules can serve both as stabilizing and reducing agents, facilitating a simple, one-step surface-directed growth. For example, tyrosine-containing peptides have been shown to be reducing agents for synthesis and stabilization of metal nanoparticles in alkaline water[15,16] or water/alcohol[17,18] solutions. It is suggested that the metal reduction occurred as a result of electron transfer mechanism from tyrosine phenolic groups, which are ionized at high pH, to the respective metal ion.[15,17] In another study, Zhou et al. used tyrosine residues of silk fibroin for growth of 45 nm core−shell colloidal gold-silk fibroin biocongugates at room temperature.[19] Recently, gold and silver nanoparticles were obtained within organogel networks comprised of tyrosine-based oligopeptides or within catechol-containing polylectrolyte multilayers.[20,21]

Compared to the studies performed in solution,[6−20] bioassisted directed assembly (including synthesis and placement) of metal nanoparticles on various surfaces received considerably less attention.[4,21−23] For example, 2D highly

* Corresponding author. E-mail: vladimir@mse.gatech.edu.
[†] Georgia Institute of Technology.
[‡] Wright-Patterson AFB.

(1) Hu, M.; Chen, J.; Li, Z.; Au, L.; Hartland, G. V.; Li, X.; Marqueze, M.; Xia, Y. *Chem. Soc. Rev* **2006**, *35*, 1084.
(2) Hodes, G. *Adv. Mater.* **2007**, *19*, 639.
(3) Harris, N.; Kohn, J. *Biomaterials Informatics*; John Wiley & Sons: Hoboken, NJ, 2007.
(4) Feldheim, D.; Eaton, B. *ACS Nano* **2007**, *1*, 154.
(5) Willner, I.; Baron, R.; Willner, B. *Adv. Mater.* **2006**, *18*, 1109.
(6) Naik, R.; Stringer, S.; Agarwal, G.; Jones, S.; Stone, M. *Nat. Mater.* **2002**, *1*, 169.
(7) Seker, U.; Wilson, B.; Dincer, S.; Kim, Il W.; Oren, E.; Evans, J.; Tamerler, C.; Sarikaya, M. *Langmuir* **2007**, *23*, 7895.
(8) Ghosh, P.; Verma, A.; Rotello, V. *Chem. Commun.* **2007**, *27*, 2796.
(9) Prozorov, T.; Mallapragada, S. K.; Narasimhan, B.; Wang, L.; Palo, P.; Nilsen-Hamilton, M.; Williams, T. J.; Bazylinski, D. A.; Prozorov, R.; Canfield, P. C. *Adv. Funct. Mater.* **2007**, *17*, 951.
(10) Slocik, J.; Moore, J.; Wright, D. *Nano Lett.* **2002**, *2*, 169.
(11) Slocik, J.; Naik, R. *Adv. Mater.* **2006**, *18*, 1988.
(12) Banerjee, I.; Regan, M. *Mater. Lett.* **2006**, *60*, 915.
(13) Reiss, B. D.; Mao, C.; Solis, D. J.; Ryan, K. S.; Thomson, T.; Belcher, A. M. *Nano Lett.* **2004**, *4*, 1127.
(14) Slocik, J. M.; Tam, F.; Halas, N. J.; Naik, R. R. *Nano Lett.* **2007**, *7*, 1054.
(15) Selvakannan, P. R.; Swami, A.; Srisathiyanarayanan, D.; Shirude, P. S.; Pasricha, R.; Mandale, A. B.; Sastry, M. *Langmuir* **2004**, *20*, 7825.
(16) Bhargava, S. K.; Booth, J. M.; Agrawal, S.; Coloe, P.; Kar, G. *Langmuir* **2005**, *21*, 5949.
(17) Si, S.; Bhattacharjee, R. R.; Banerjee, A.; Mandal, T. K. *Chem.−Eur. J.* **2006**, *12*, 1256.
(18) Bhattacharjee, R. R.; Das, A. K.; Haldar, D.; Si, S.; Banerjee, A.; Mandal, T. K. *J. Nanosci. Nanotechnol.* **2005**, *5*, 1141.
(19) Zhou, Y.; Chen, W.; Itoh, H.; Naka, K.; Ni, Q.; Yamaneb, H.; Chujo, Y. *Chem. Commun.* **2001**, 2518.
(20) Ray, S.; Das, A. K.; Banerjee, A. *Chem. Commun.* **2006**, 2816.
(21) Lee, H.; Lee, Y.; Statu, A.; Rho, J.; Park, T.; Messersmith, P. *Adv. Mater.* **2008**, *20*, 1619.
(22) Gorna, K.; Munoz-Espi, R.; Groehn, F.; Wegner, G. *Macromol. Biosci.* **2007**, *7*, 163.

10.1021/cm801475v CCC: $40.75
Published on Web 08/21/2008

organized nanostructures were obtained by deposition of preformed colloids of nanoparticles on biomolecular pretreated surfaces.[24] The method allows for control over particle orientation and specific formation on the designed sites. Another principle involves application of in situ nanoparticle formation on prepared substrates modified with biomolecules. For example, silver or gold microprinting was applied to peptide- or chitosan-modified surfaces.[6,23] Some other examples on biomimetic organization in situ include RNA-[25] or DNA-based "molecular lithography"[26] as well as virus,[27] fungus,[28] or silk fiber-templated[29] reduction of gold and silver nanostructures. However, despite the increasing interest in using organic substrates or living organisms for formation of metal nanoparticles, the controllable surface-mediated nanoparticle nucleation and growth still remains a challenge. A facile, robust, and cost-effective method should be developed to direct the growth and easy transfer of metal nanoparticles to various surfaces for potential applications as optoelectronic devices, pressure, humidity, photothermal, or magnetic sensors, as well as in drug delivery, catalysts, and antimicrobial coatings.[30−34]

In this paper, we report on preparation of redox-active nanoscale layer-by-layer (LbL) films [35−40] with polyaminoacid-decorated surfaces that serve for nucleation and growth of uniformly distributed gold nanoparticles at ambient conditions. In contrast to the previously utilized short-chain tyrosine oligopeptides,[15,17,18] which showed reducing activities in solutions, here we introduce a poly-L-tyrosine (pTyr), a long-chain synthetic polyaminoacid, as a nucleator and stabilizer for gold particles. In addition, we study its reducing activity after its deposition on the surface of LbL films from different solvents on different types of substrates. To the best of our knowledge, this is the first attempt to apply pTyr to a solid surface in order to provide in situ formation of individual gold nanoparticles.

Specifically, we found that pTyr as an organic template is able to direct nanoparticle formation to solid, flexible, and patterned surfaces, thus preventing particle agglomeration and precipitation from solutions which usually occurs if conventional reducing solution methods are used.[1,41] Advantages of using pTyr, instead of short-chain synthetic oligopeptides[15,17,18] and amino acids,[16] include its compatibility with conventional LbL techniques, availability, modest cost, biocompatibility, and easy processability, all of which are crucial for various demanding applications. The reported results on bioinspired gold formation can be readily expanded to any inorganic-selective surface and provide a simple, robust, and nontoxic method to obtain nonaggregated inorganic nanoparticles at ambient conditions.

Experimental Section

Materials. Poly(allylamine hydrochloride) (PAH, $M_W = 65\,000$), poly(sodium 4-styrenesulfonate) (PSS, $M_W = 70\,000$), poly-L-tyrosine (pTyr, $M_W = 10\,000-40\,000$), cellulose acetate (50 000), borate buffer (pH 10), and $HAuCl_4$ solution were purchased from Aldrich.

Instrumentation. Polypeptide deposition and gold formation were studied by Dimension 3000 AFM microscope (Digital Instruments). AFM images were collected in the tapping mode with silicon tips with a spring constant of 50 N/m. The thicknesses of the pTyr layer and underlying (PAH/PSS) layers were measured with a spectroscopic ellipsometer M2000U (Woolam). TEM was performed with a JEOL 100CX-2 electron microscope at 100 kV. High-resolution TEM (HRTEM) images were obtained on Hitachi HD-2000 Field Emission Gun (FEG) TEM at 200 kV. EDAX spectra were collected on a Phillips CM200 TEM Lab6 operating at 200 kV equipped with a Thermo Electron EDAX detector. UV−vis spectra were recorded on a CARY spectrophotometer using quartz slides as templates.

Multilayer Deposition and Formation of Gold Nanoparticles. Multilayered films were obtained by alternating deposition of poly(allylamine hydrochloride) (PAH) and poly(styrene sulfonate) (PSS) polyelectrolytes by spin-assisted LbL (SA-LbL) method, which is a combination of spin coating and conventional LbL techniques.[42,43] Specifically, 30 μL of 1 mg/mL polyelectrolyte solutions were sequentially dropped on silicon substrates and rotated for 20 s with a 5000 rpm rotation speed, rinsing twice with Nanopure water between the deposition cycles, starting from PAH. Thus, 2-bilayer $(PAH\text{-}PSS)_2$ or 2.5-bilayer $(PAH\text{-}PSS)_2PAH$ films were constructed. Free-standing films were fabricated by initial deposition of a sacrificial layer of acetate cellulose from 2% solution in dioxane followed by 20-bilayer (PSS-PAH) LbL assembly. pTyr ($M_W = 40$ kDa) was then deposited from 1 mg/mL aqueous at pH 10.5 or ethanol/water (50/50) solutions on a surface of PAH-terminated $(PAH\text{-}PSS)_2PAH$ or PSS-terminated $(PAH\text{-}PSS)_2$ film. Unbound pTyr was then removed by extensive rinsing with borate buffer at pH 10.5 or ethanol/water (50/50) solutions. The deposition of the pTyr was monitored by AFM and ellipsometry. Free standing films were released from silicon substrates by exposure to acetone. Formation of gold particles was achieved by immersing the polyelectrolyte-pTyr films into 1 mM $HAuCl_4$ solution at room temperature in 0.1 M borate buffer at pH 10.5 followed by extensive rinsing with Nanopure water.

(23) Wang, B.; Chen, K.; Jiang, S.; Reincke, F.; Tong, W.; Wang, D. Gao. *Biomacromolecules* **2006**, *7*, 1203.
(24) Hall, S.; Shenton, W.; Engelhardt, H.; Mann, S. *Chem. Phys. Chem.* **2001**, *2*, 184.
(25) Gugliotti, L. A.; Feldheim, D. L.; Eaton, B. *J. Am. Chem. Soc.* **2005**, *127*, 17814.
(26) Keren, K.; Krueger, M.; Gilad, R.; Ben-Yoseph, G.; Sivan, U.; Braun, E. *Science* **2002**, *297*, 72.
(27) Dujardin, E.; Peet, C.; Stubbs, G.; Culver, J.; Mann, S. *Nano Lett.* **2003**, *3*, 413.
(28) Ahmad, A.; Senapati, S.; Khan, M. I.; Kumar, R.; Sastry, M. *J. Biomed. Nanotechnol.* **2005**, *1*, 47.
(29) Dong, Q.; Su, H.; Zhang, D. *J. Phys. Chem. B* **2005**, *109*, 17429.
(30) Wang, T.; Rubner, M.; Cohen, R. *Langmuir* **2002**, *18*, 3370.
(31) Schuets, P.; Caruso, F. *Chem. Mater.* **2004**, *16*, 3066.
(32) Nohria, R.; Khillan, R.; Su, Y.; Kikshit, D.; Lvov, Y.; Varahramyan, K. *Sens. Actuators, B* **2006**, *114*, 218.
(33) Jiang, C.; McConney, M. E.; Singamaneni, S.; Merrick, E.; Chen, Y.; Zhao, J.; Zhang, L.; Tsukruk, V. *Chem. Mater.* **2006**, *18*, 2632.
(34) Dai, J.; Bruening, M. *Nano Lett.* **2002**, *2*, 497.
(35) Decher, G. *Science* **1997**, *277*, 1232.
(36) *Protein Architecture: Interfacing molecular Assembly and Immobilization Biotechnology*; Lvov, Y., Mohwald, H. Eds.; Marcel Dekker: New York, 2000.
(37) Lvov, Y.; Decher, G.; Möhwald, H. *Langmuir* **1993**, *9*, 481.
(38) Hiller, J.; Mendelsohn, J. D.; Rubner, M. F. *Nat. Mater.* **2002**, *1*, 59.
(39) Tang, Z.; Kotov, N. A.; Magonov, S.; Ozturk, B. *Nat. Mater.* **2003**, *2*, 413.
(40) Tsukruk, V. V. *Prog. Polym. Sci.* **1997**, *22*, 2477.
(41) Evanoff, D.; Chumanov, G. *ChemPhysChem* **2005**, *6*, 1221.
(42) Jiang, C.; Markutsya, S.; Pikus, Y.; Tsukruk, V. *Adv. Mater.* **2004**, *16*, 157.
(43) Markutsya, S.; Jiang, C.; Pikus, Yu.; Tsukruk, V. V. *Adv. Funct. Mater.* **2005**, *15*, 771.

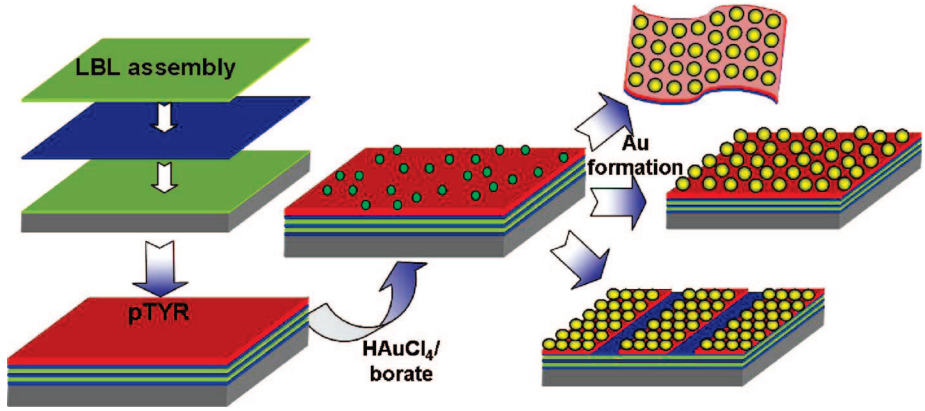

Figure 1. Schematic presentation of pTyr-induced surface-mediated synthesis of gold nanoparticles on planar solid and flexible substrates in uniform and micropatterned manners.

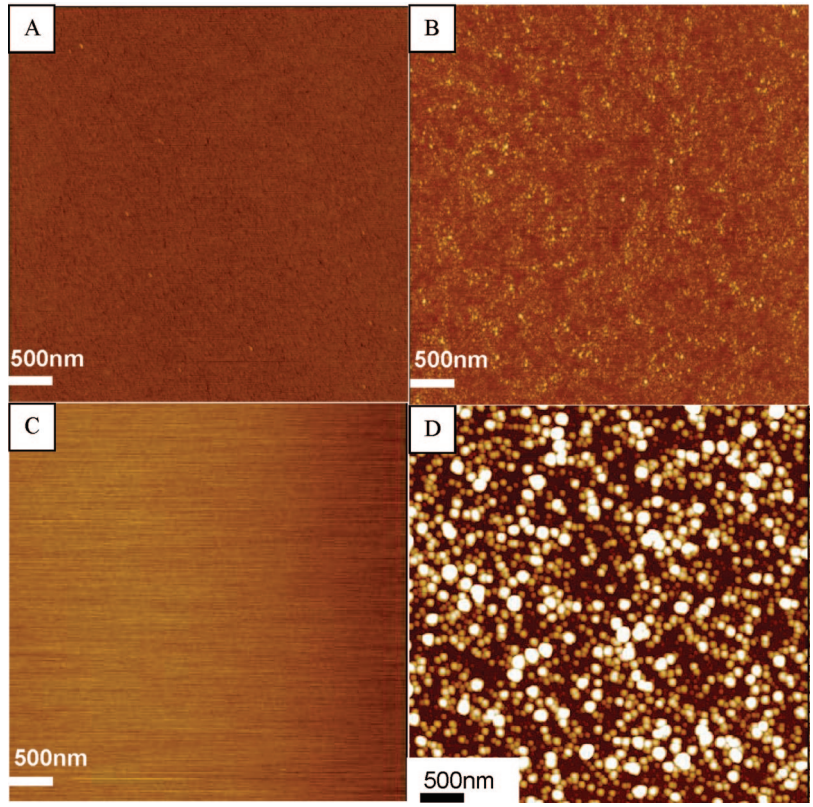

Figure 2. (A, B) AFM images of a $(PAH\text{-}PSS)_2$ film (A) and $(PAH\text{-}PSS)_2$pTyr film with topmost pTyr layer deposited from a water/alcohol solution (B) before exposure to $HAuCl_4$. (C, D) AFM images of the $(PAH\text{-}PSS)_2$ (C) and $(PAH\text{-}PSS)_2$pTyr (D) films exposed to $HAuCl_4$ solution for 5 days. Z-scale is 10 nm (A–C) and 40 nm (D).

Results and Discussions

The scheme of fabrication of pTyr-decorated LbL films on different templates and their further reduction is shown in Figure 1. Specifically, pTyr was allowed to adsorb on polyelectrolyte LbL templates prefabricated with spin-assisted LbL technique. pTyr-assisted reduction of gold nanoparticles was then achieved by immersing the LbL-pTyr films into a 1 mM $HAuCl_4$ solution at room temperature under mild alkaline conditions (0.1 M borate buffer at pH 10.5) to ionize tyrosine groups (pI = 11.4[44]) and make them capable of further electron transfer.

We found that pTyr can be successfully deposited onto PSS-terminated LbL assembly from water/ethanol with the thickness of 2.5 ± 0.2 nm. Specifically, AFM analysis of $(PAH\text{-}PSS)_2$ films before (Figure 2a) and after (Figure 2b) pTyr deposition reveals increase in surface microroughness from 0.25 to 0.75 nm. Further exposure of pTyr-LbL films to $HAuCl_4$/borate solution for 5 days results in formation of gold nanoparticles with a diameter distribution from 10 to 36 nm confined to the topmost layer (Figure 2d). The AFM image shows that the nanoparticles are uniformly distributed over the surfaces without any large aggregates (Figure 2d). In contrast, $(PAH\text{-}PSS)_2$ films without the pTyr layer remain smooth and uniform and did not show any particles on the surface after the identical exposure (Figure 2c).

(44) Senior, M.; Gorrell, S.; Hamori, E. *Biopolymers* **1971**, *10*, 2387.

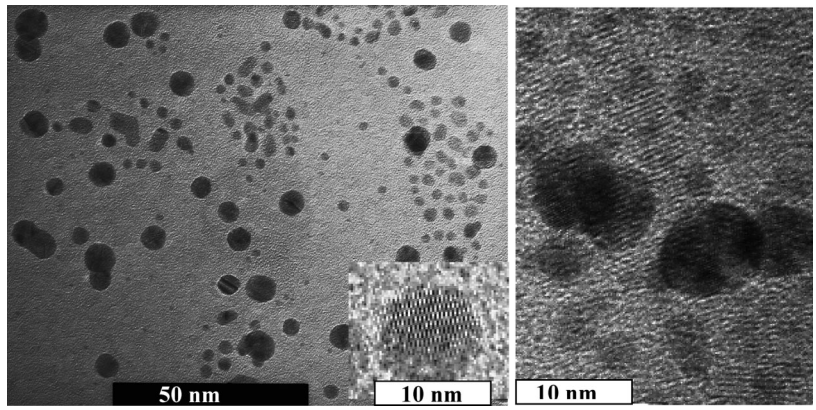

Figure 3. HRTEM images of $(PAH\text{-}PSS)_2pTyr$ films exposed to $HAuCl_4$ for 5 days.

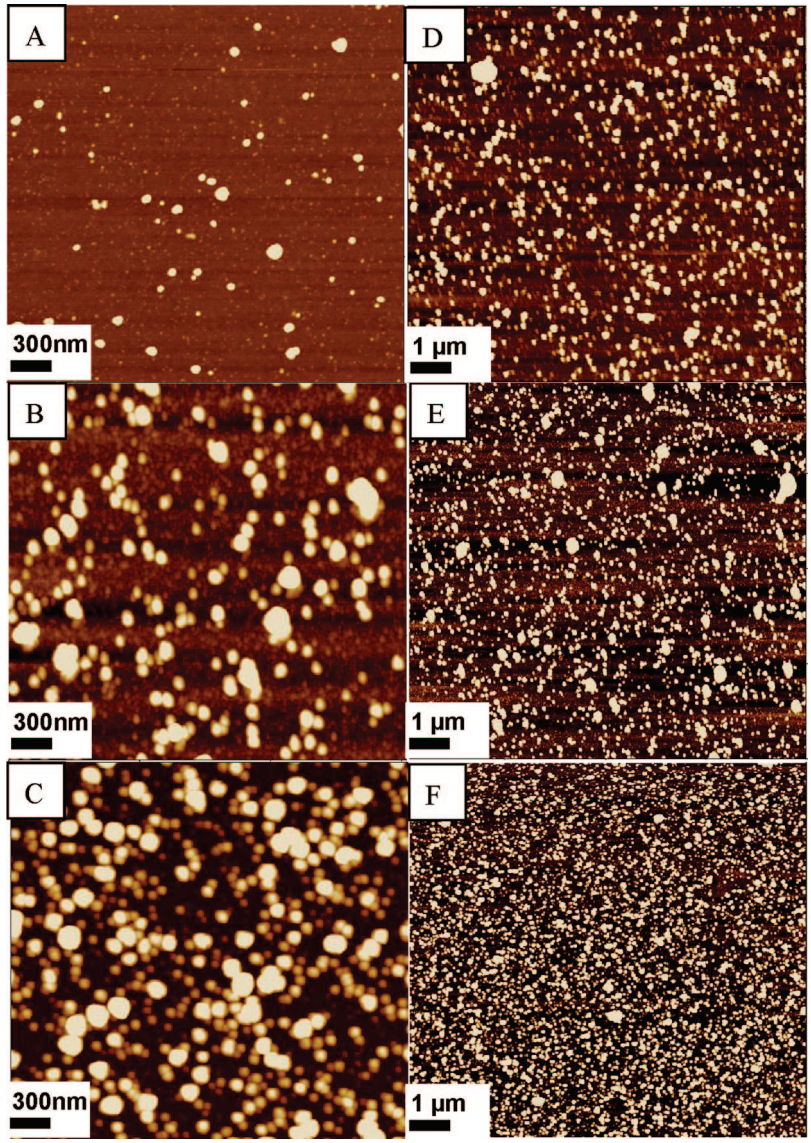

Figure 4. AFM images of $(PAH\text{-}PSS)_2pTyr$ films exposed to $HAuCl_4$ for (A, D) 1 day, (B, E) 2 days, and (C, F) 5 days. Z-scale is (A, D− F) 20 and (B, C) 40 nm. Scan size is (A−C) 3 × 3 and (D−F) 10 × 10 μm^2.

A close look at the nanoparticle sizes calculated from AFM images revealed that the gold nanoparticles possess rather broad diameter distribution with the majority of the nanoparticles of 18 ± 7 nm in diameter and with the smaller fraction (∼15%) of larger nanoparticles with the diameter of 50 ± 8 nm. The formation of tyrosine-reduced metal nanoparticles with broad distribution was earlier observed in solutions.[16,17] In that case, Au nanoparticles

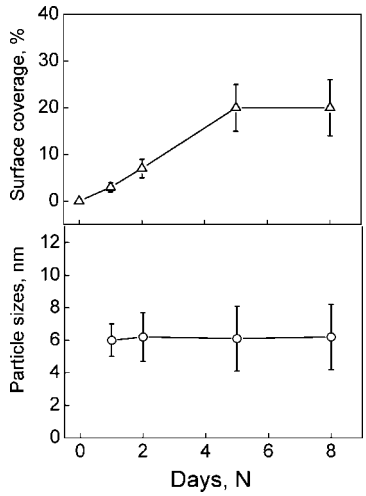

Figure 5. Time evolution of particle surface coverage (top panel) and particle sizes (bottom panel).

of very small (several nanometer) diameter are referred to nanoparticle nuclei with nuclei coagulation resulting into larger nanoparticles.[16]

The size of the nanoparticle was then obtained from TEM and HRTEM images. For that purpose pTyr-LbL films were released from original substrates (silicon wafers) as free-suspended films by dissolving sacrificial layer in accordance with usual procedure.[45] TEM analysis of these films suspended on TEM grids confirmed the uniform surface distributions of gold nanoparticles with an average diameter of 8 ± 2 nm, which was significantly smaller that that found from AFM images. We suggest that the larger particles dimensions observed with AFM indicate the presence of organic material around the particles invisible on HRTEM images and will be discussed below. In addition, HRTEM showed that the most of the particles have spherical shape but also revealed the presence of very small species of 2 ± 0.5 nm in diameters (Figure 3). The presence of the small particles indicates that the mechanism of the surface-mediated nanoparticle reduction is similar to that found in solutions when L-tyrosine-induced reduction results in initial formation of the nanoparticles nuclei of 0.7−1.5 nm in diameters and their further aggregation into the larger nanoparticles with diameters of 5−40 nm.[16] Lattice fringes found on both large and small particles indicate their crystalline structure with parameters observed for gold nanoparticles of similar dimensions (inset and right panel in Figure 3).

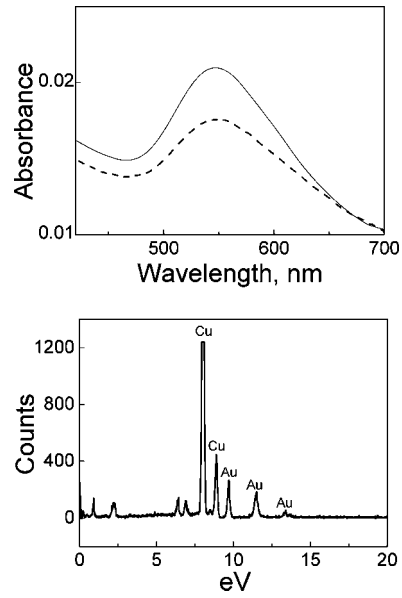

Figure 7. UV and EDX of Au nanoparticles grown on pTyr-tethered LbL surfaces. Solid and dashed lines in UV spectra represent gold nanoparticles grown on pTyr layer fabricated from aqueous pH 10 and water/alcohol solutions, respectively. EDX was obtained for free-standing $(PAH/PSS)_{20}$ pTyr-Au film (pTyr was deposited from water/alcohol solution) transferred to Cu grids.

We further studied the surface-provided nucleation and growth by controlling surface coverage by varying time allowed for their formation. AFM analysis of nanoparticle surface density as a function of time demonstrates that amount of particles increased with increasing time allowed for the reduction (Figure 4). Specifically, surface coverage gradually increased to 20% but became saturated with further increase in the reduction time (Figure 5). Interestingly, there is no significant effect of the reduction time on the average nanoparticle size indicating confinement conditions imposed by the topmost polyamino-acid layer on the ripening process (Figure 5). TEM data also independently showed that exposure of the pTyr modified substrates into reduction solution for 2 and 5 days resulted in an increase in the amount of nanoparticle on the surfaces (Figure 6).

The pTyr-mediated formation of gold nanoparticles on flat and flexible substrates was also confirmed by EDX analysis and UV-spectroscopy (Figure 7). The EDX spectrum of these films showed three characteristic bands for gold confirming the composition of nanoparticles observed in AFM and TEM

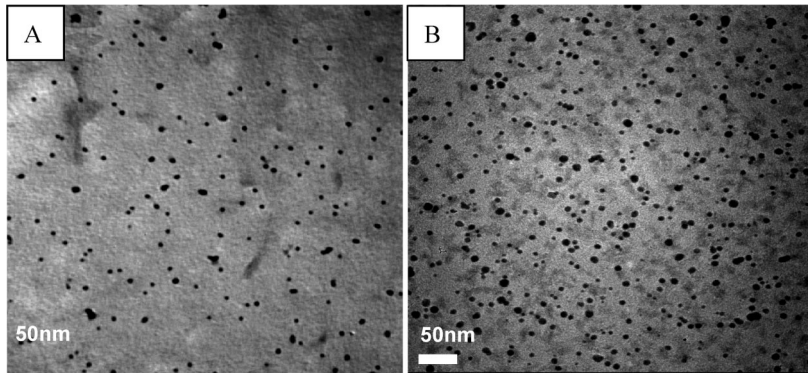

Figure 6. TEM images of $(PAH\text{-}PSS)_2$pTyr films exposed to $HAuCl_4$ for (A) 2 and (B) 5 days.

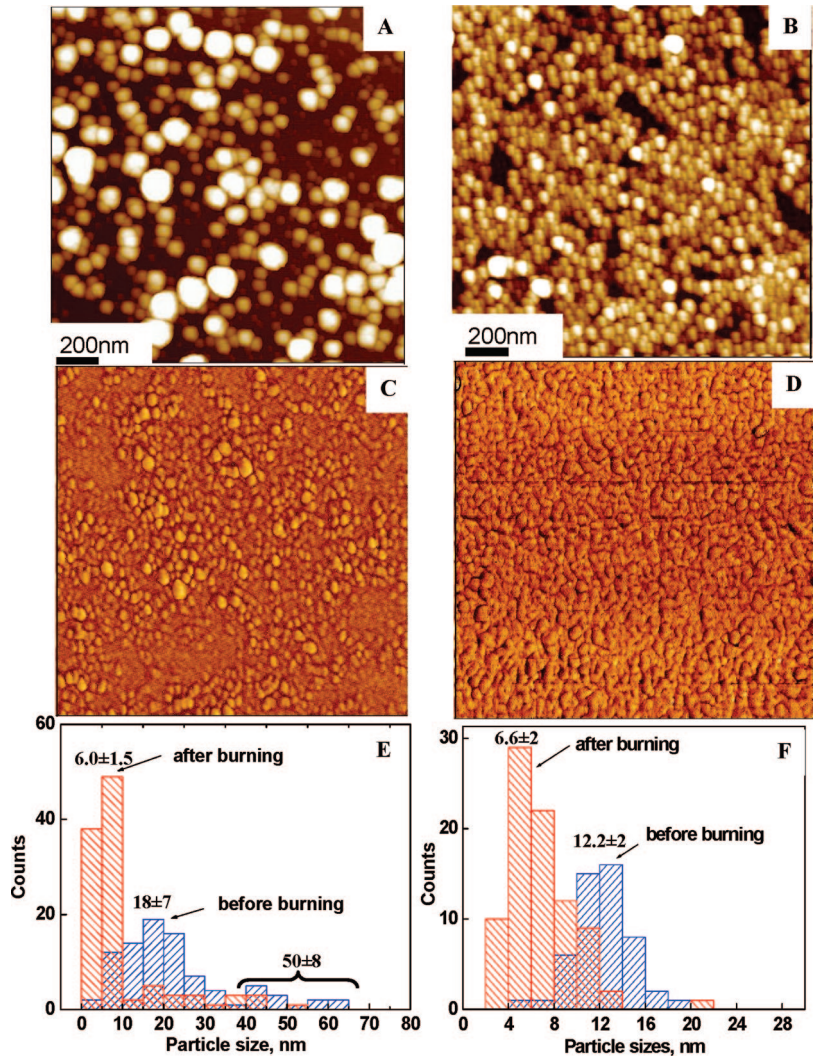

Figure 8. (A, B) AFM topography and (C, D) phase images of Au nanoparticles grown on pTyr-decorated LbL surface when pTyr was deposited (A) from water/alcohol solutions or (B) from aqueous solutions at pH 10.5. Z-scale is (A) 60 and (B) 20 nm. Scan size is 2 × 2 μm^2. (E, F) The histograms of nanoparticle diameters before and after temperature treatment are calculated from AFM data.

images (Figure 7). Moreover, the gold nanoparticles on pTyr-LbL films showed distinctive UV absorption with a broad maximum centered at 547 nm (Figure 7). The position of this peak indicates the presence of individual gold nanoparticles with diameter below 50 nm, in accordance with literature data.[23] The modest red-shift observed in this case is caused by variable dielectric environment for nanoparticles directly localized on the surface layer.[46]

Our next study was focused on exploring the effect of pTyr deposition conditions on nanoparticle formation. For that purpose, we prepared the topmost pTyr layer from pure aqueous solution at pH 10.5, instead of water/alcohol solution. Deposition of pTyr at pH 10.5 was performed on a positively charged PAH-terminated surface to provide adhesion to the negatively charged tyrosine groups. Surprisingly, under these conditions, we observed the formation of densely packed gold nanoparticles with the surface coverage reaching 450 nanoparticles/μm^2 or about 40% higher than that for that obtained from water/alcohol solution (compare images A and B in Figure 8). Moreover, the nanoparticles looked smaller and showed the uniform size distribution with the average diameter of 12.2 ± 2 nm, well below that discussed above (panels E and F in Figure 8). The higher surface coverage in the case of pTyr deposited from pH 10.5 was also confirmed by UV analysis. The UV spectrum shows absorption band at 547 nm similarly to the previous case but with the higher absorption, which represents a higher nanoparticle concentration on the surface (Figure 7a).[17,23]

We suggest that the difference in surface coverage can be related to different surface morphology of pTyr layers deposited from aqueous at pH 10.5 and water/alcohol solutions. Figure 9 compares high-resolution AFM (HRAFM) for pTyr-free polylectrolyte films with pTyr deposited at different conditions. The data reveals that the films deposited from aqueous solutions have lower microroughness compared to those from water/alcohol solutions. Indeed, as a result of pTyr interaction with the underlying PAH layer, a film with a roughness of 0.6 nm and thickness of 2.0 ± 0.2 nm was obtained (images E and F in Figure 9), which was slightly thinner, but smoother as compared to the film deposited from

(45) Mamedov, A. A.; Kotov, N. A. *Langmuir* **2000**, *16*, 5530.
(46) Wang, B.; Chen, K.; Jiang, S.; Reince, F.; Tong, W.; Wang, D.; Gao, C. *Biomacromolecules* **2006**, *7*, 1203.

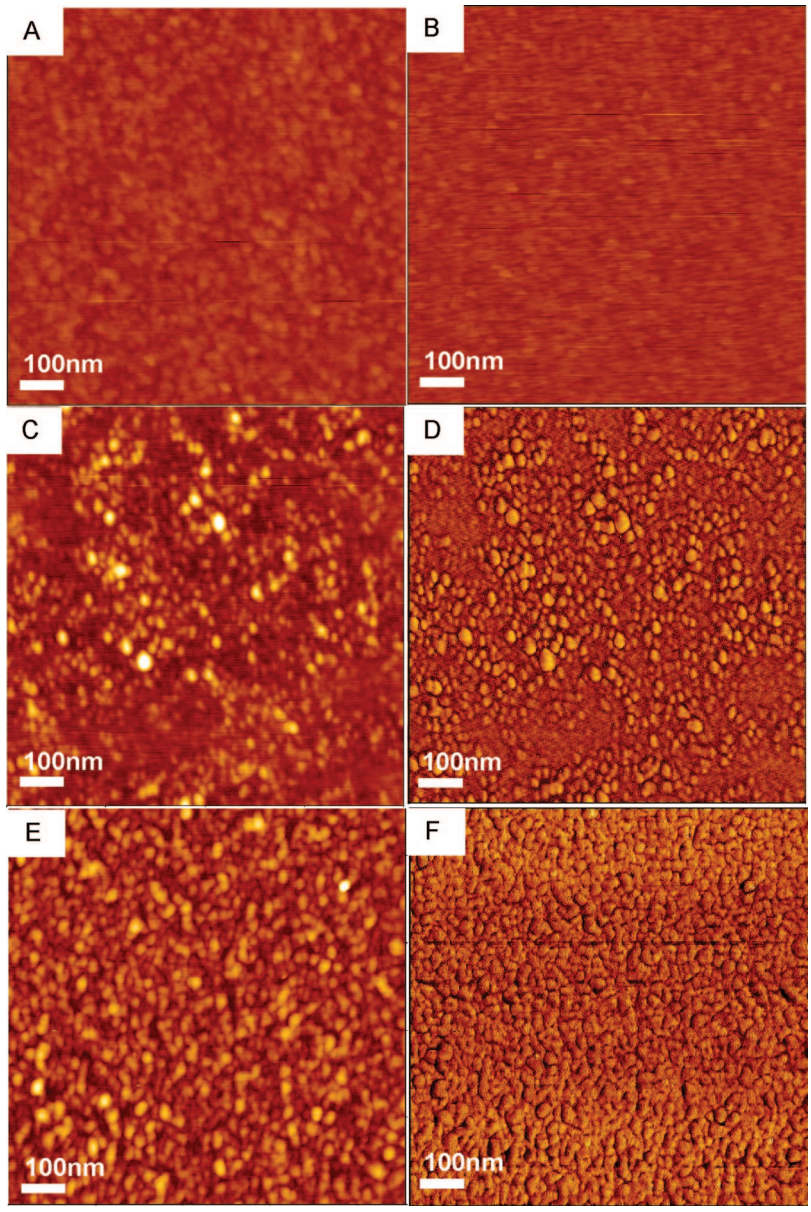

Figure 9. (A−C, E) High-resolution AFM topography images of $(PAH\text{-}PSS)_2$ film (A) before and (B) after exposure to $HAuCl_4$; and $(PAH\text{-}PSS)_2$pTyr films before exposure to $HAuCl_4$ with pTyr deposited (C) from water/alcohol solutions or (E) from aqueous solutions at pH 10.5. Phase images of C and E are presented as D and F, respectively. Scan size is 1×1 μm^2. Z-scale is 10 nm.

water/alcohol solution which was of 0.75 nm and 2.5 ± 0.2 nm in roughness and thickness, respectively (images C and D in Figure 9). Cross-sectional analysis of the images shows that the surface of pTyr deposited from pH 10.5 is uniform with no evidence of surface aggregates (Figure 10A). However, a pTyr layer formed from water/alcohol solutions shows some surface domains irregular in size, and leads to the higher surface microroughness. Specifically, sectional analysis of the surface indicates that the domains range in heights from 2 to 5 nm with lateral dimensions of 15−45 nm yielding in the protein domain volumes of 250−750 nm^3, as was quantified from AFM data after correction of the tip dilation[47] (panels B and C in Figure 10).

We suggest that the observed difference in surface morphology of the pTyr layer fabricated at different conditions might be caused by different "globular" and "necklace" conformations of hydrophobic polymer chains, earlier found for polymer solutions.[48] Indeed, according to the theoretical consideration, pTyr ($pI = 11.4$) as a neutral hydrophobic molecule at pH <10.5 was shown to collapse into dense spherical "globules" in ethanol/water solutions to maximize the number of favorable polymer−polymer contacts and form intra- and interhydrogen bonding complexes in alcohol solution.[49] These "globules", preformed in solution, lead to the formation of the surface domains. Considering a molecular volume of a single pTyr molecule of ~40 000 Da in a condensed state is 65 nm^3 and that the volumes of domain adsorbed from water/alcohol solutions is of 250−750 nm^3,

(47) Ornatska, M.; Peleshanko, S.; Genson, K. L.; Rybak, B.; Bergman, K. N.; Tsukruk, V. V. *J. Am. Chem. Soc.* **2004**, *126*, 9675.

(48) Dobrynin, A. V.; Rubinstein, M. *Prog. Polym. Sci.* **2005**, *30*, 1049.

(49) Hunt, N. T.; Turner, A. R.; Wynne, K. *J. Phys. Chem. B* **2005**, *109*, 19008.

(50) Sperling, L. H. *Introduction to Physical Polymer Science*; Wiley & Sons: Hoboken, NJ, 2006.

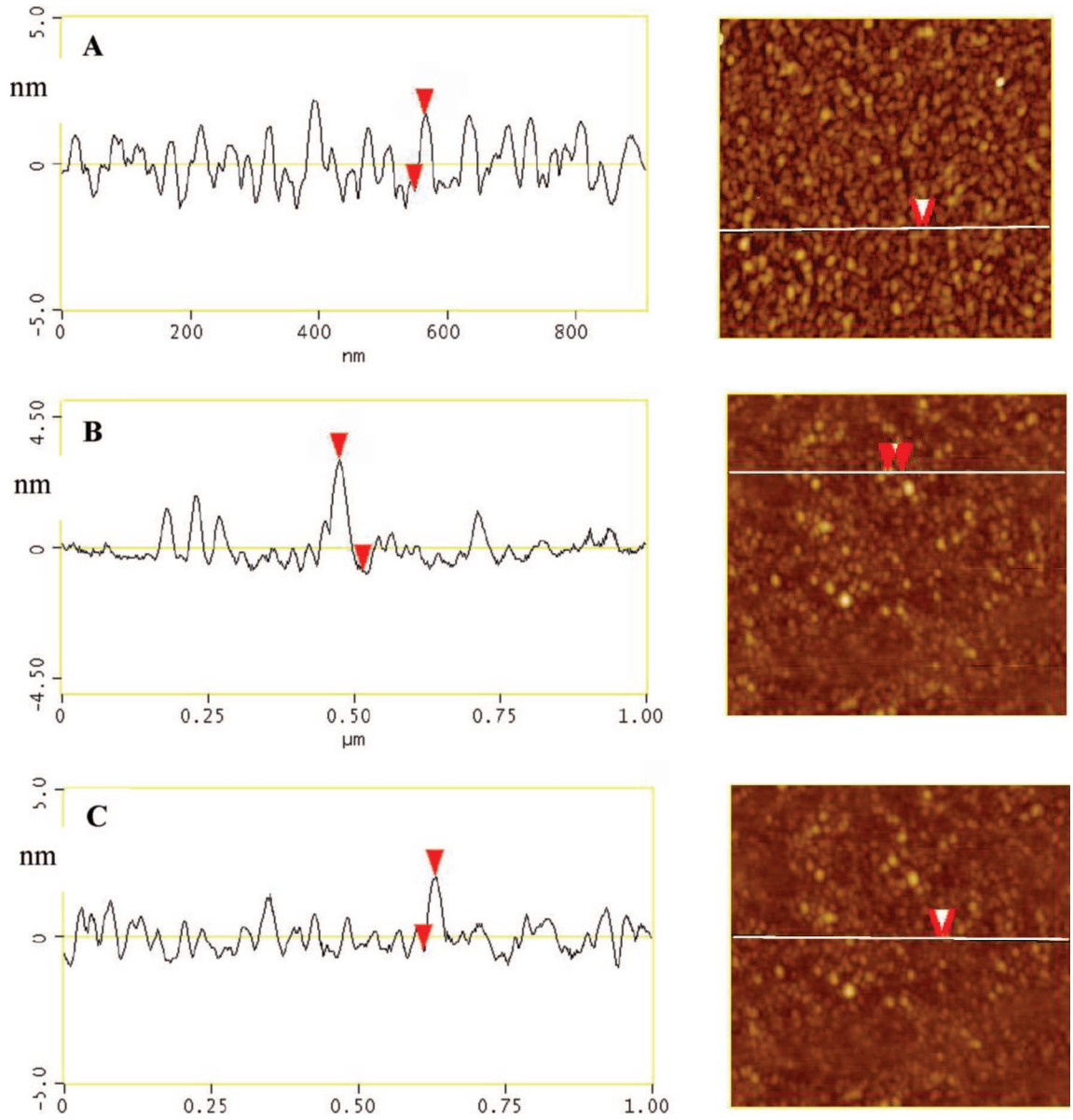

Figure 10. Cross-sectional analysis of 1 × 1 μm^2 AFM images of $(PAH\text{-}PSS)_2pTyr$ films with pTyr deposited (A) from aqueous solutions at pH 10.5 or (B, C) from water/alcohol solutions at two different cross-section areas.

we can conclude that a single pTyr domain in the dry state is comprised of 4−11 pTyr molecules.[50] In other words, this kind of surface morphology presented in pTYR domains of different sizes is responsible for further nucleation and growth of gold nanoparticles, the sizes and distribution of which follow the pattern of the domain sizes and distributions. On the other side, pTyr grainy surface morphology prevents the formation of large aggregates because the growing gold nanoparticles are confined to the interior of pTYR domains. In contrast, pTyr chains being partially ionized at pH ≥ 10.5 might form "necklaces" with identical beads stabilized by the negative charges and evenly distributed over the surface. Thus, we believe that in the case of pTyr layer fabricated from aqueous solutions, the pTyr beads can initiate growth of gold nanoparticles with the high surface coverage and uniform size distribution.

It is worth noting that no morphological changes are observed with PSS-terminated film after its exposure to the reducing solution for 5 days, thus excluding synthetic LbL substrate from the growth process (images A and B in Figure 9). On the other hand, PAH-terminated film showed reducing activity at these conditions but with the very pronounced nanoparticle coagulation into clusters of tenth microns across (Figure 1S in the Supporting Information). The results indicates that the additional coating of PAH-tethered films with pTyr layer promote formation of gold particles of high monodispersity and more uniform surface coverage.

Considering that the nucleation and growth of Au nanoparticles occurs within pTyr surface layer swollen in a good solvent, one can expect that nanoparticles are surrounded by pTyr, similarly to that observed in solution.[15,17] In fact, the core−shell structure was confirmed by phase AFM images showing the low contrast that can be attributed to uniform chemical composition caused by complete coverage with synthetic polyami-

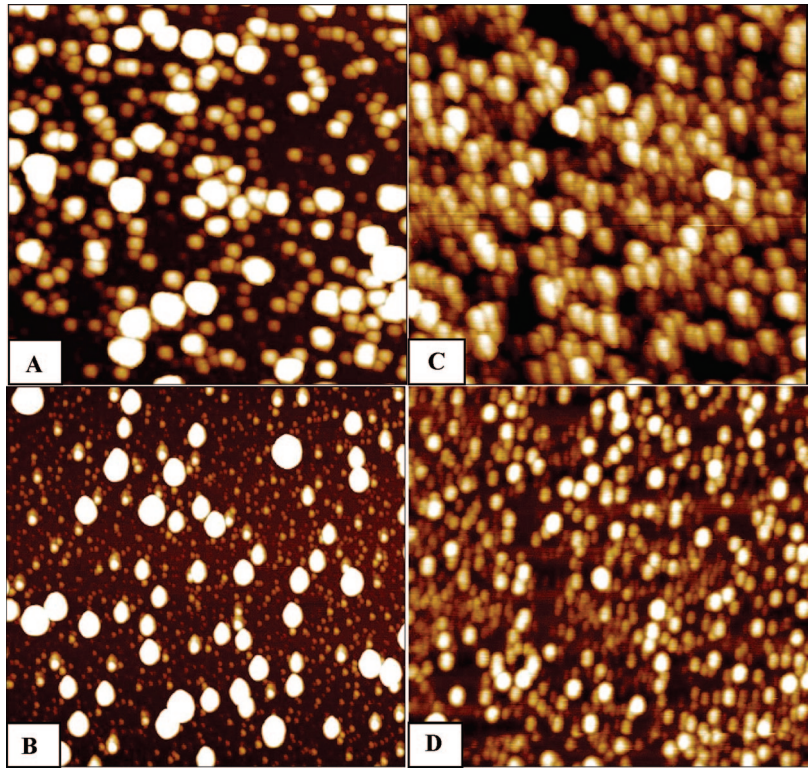

Figure 11. AFM images of Au particles reduced on a pTyr-tethered surface (pTyr was deposited from water/alcohol solutions) (A) before and (B) after treatment with 600 °C; or from solutions at pH 10.5 (C) before and (D) after treatment with 600 °C. Scan size is (a, b) 2 × 2 μm^2 and (c, d) 1 × 1 μm. Z-scale is (A) 60, (B) 30, and (C, D) 10 nm.

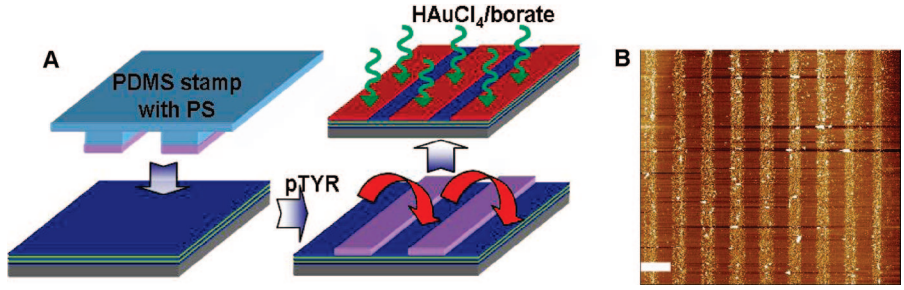

Figure 12. (A) Schematic and (B) AFM image of Au nanoparticles grown on a micropatterned pTyr-LbL surface. The micropatterned polyelectrolyte template was prepared by polystyrene (PS) stamping onto $(PAH/PSS)_2$ LbL film, followed by pTyr deposition from water/alcohol solution, PS dissolution in toluene, and exposure to $HAuCl_4$/borate for 5 days. For the AFM image, Z-scale is 60 nm and scale bar is 10 μm.

noacid.[51] Thus, to determine the actual nanoparticle size, Au-pTyr-LbL specimens were treated at 600 °C for 1 h to remove all organic components. This temperature treatment revealed that the nanoparticles significantly "shrink" and showed more uniform size distribution. Specifically, for a water/alcohol system, the average size of the fairly uniform fine Au nanoparticles without pTyr shells was 6.0 ± 1.5 nm, which is ~12 nm smaller than the original size (18 ± 7nm) before heat treatments (Figure 8E and images A and B in Figure 11). Such a difference indicates the presence of pTyr shell of ~6 nm around the Au core. The result correlates fairly well with nanoparticle dimensions (8 ± 2 nm) found from TEM analysis. Similarly, for assembly from aqueous solution, removing the organic material resulted in the average diameter of 6.6 ± 2 nm, suggesting the presence of pTyr shell of ~3 nm (Figure 8F and images C and D in Figure 11).

Furthermore, to explore whether the above method of directed assembly of Au nanoparticles can be utilized for their control placement within selected surface areas of LbL templates, we fabricated micropatterned pTyr-LbL surface by placing periodic 3 μm sacrificial PS stripes by using capillary transfer lithography as discussed earlier (Figure 12).[52,53] Micropatterned pTyr-LbL assembly was exposed to a reducing solution followed by removal of PS protective stripes. As a result of this selective assembly, we observed a micropatterned distribution of gold nanoparticles exclusively grown on pTyr-terminated surface areas of the original striped LbL template with 10 μm spacing (Figure 12). This example shows high selectivity of the growth process

(51) Luzinov, I.; Julthongpiput, D.; Tsukruk, V. V. *Macromolecules* **2000**, *33*, 7629.

(52) Ko, H.; Jiang, C.; Tsukruk, V. V. *Chem. Mater.* **2005**, *17*, 5489.

suggested here and opens the path for easy, facile, and robust assembly of metal nanoparticles on or within the LbL templates.

In conclusion, we showed that pTyr deposited either from alcohol or aqueous solutions was able to initiate formation of gold nanoparticles onto solid, flexible, or patterned surfaces. The 8 nm gold particles were surrounded by 3−6 nm polyaminoacid shell and confined to the topmost polyaminoacid layer. It is worth noting that the flexible nanoparticle-containing LbL films can be easily transferable to any solid substrates without multistep processes of solution growth, purification, and casting.

Acknowledgment. This work was supported by funding provided by the Air Office of Scientific Research and the Office of Naval Research. The authors thank Yolande Berta for HRTEM work and Hyunhyub Ko for technical assistance.

Supporting Information Available: Additional figure (PDF). This material is available free of charge via the Internet at http://pubs.acs.org.

CM801475V

(53) Jiang, C.; Markutsya, S.; Shulha, H.; Tsukruk, V. V. *Adv. Mater.* **2005**, *17*, 1669.